

BEST PRACTICE IN NUMERICAL SIMULATION AND CFD BENCHMARKING. RESULTS FROM THE SUSANA PROJECT

Tolias, I.C.¹, Giannissi, S.G.¹, Venetsanos, A.G.¹, Keenan, J.², Shentsov, V.², Makarov, D.², Coldrick, S.³, Kotchourko, A.⁴, Ren, K.⁴, Jedicke, O.⁴, Melideo, D.⁵, Baraldi, D.⁵, Slater, S.⁶, Duclos, A.⁷, Verbecke, F.⁷ and Molkov, V.²

¹ Environmental Research Laboratory, National Center for Scientific Research Demokritos, Agia Paraskevi, 15310, Greece, tolias@ipta.demokritos.gr

² HySAFER Centre, Ulster University, Newtownabbey, BT37 0QB, UK, dv.makarov@ulster.ac.uk

³ Health and Safety Executive, Harpur Hill, Buxton, SK17 9JN, UK, Simon.Coldrick@hsl.gsi.gov.uk

⁴ Karlsruhe Institute for Technology (KIT), Kaiserstrasse 12, Karlsruhe, Germany, olaf.jedicke@kit.edu

⁵ European Commission, Joint Research Centre (JRC), IET, Westerduinweg 3, 1755 LE, Petten, Netherlands, daniele.baraldi@ec.europa.eu

⁶ Element Energy Limited, Station Road 20, Cambridge, United Kingdom, shane.slater@element-energy.co.uk

⁷ Areva Stockage d'Energie SAS, Batiment Jules Verne, Domaine du Petit Arbois, Aix-en-Provence, France, audrey.duclos@areva.com

ABSTRACT

A comprehensive guide to Best Practice Guidelines (BPG) in numerical simulations for Fuel Cells and Hydrogen applications has been one of the main outputs of the SUSANA project. These BPG focus on the practical needs of engineers in consultancies and industry undertaking Computational Fluid Dynamics (CFD) simulations or evaluating CFD simulation results in support of hazard/risk assessments of hydrogen facilities, and the needs of regulatory authorities. This contribution presents the BPG document and the BPG application through a series of CFD benchmarking examples.

1.0 INTRODUCTION

One of the main objectives of the SUSANA project¹ was to develop comprehensive Best Practice Guidelines (BPG) in numerical simulations for Fuel Cells and Hydrogen (FCH) applications. These BPG focus on the practical needs of engineers in consultancies and industry undertaking Computational Fluid Dynamics (CFD) simulations or evaluating CFD simulation results in support of hazard/risk assessments of hydrogen facilities, and the needs of regulatory authorities. The reader of the BPG document is introduced to the appropriate modelling approaches, in order to improve the accuracy of their modelling and the quality of hydrogen-safety simulations.

A number of BPG for CFD applications are available. ERCOFTAC developed a general BPG for industrial CFD simulations [1]. BPG for CFD simulations that focus on specific applications have also been developed, for example for flows in urban environments [2]. In the context of risk assessments for FCH technology and applications, one may face the need to simulate whole range of physical phenomena and accident scenarios which follow an unexpected hydrogen leak – release, ignition, fire, deflagration and detonation. This need was taken into consideration in developing the BPG in numerical simulations for FCH applications.

In this paper, a summary of the SUSANA BPG and some applications are presented. The reader can consult the complete guide [3] and the reports on benchmark activities [4], [5] for more details. The BPG are separated into Sections based on the studied phenomena: hydrogen releases and dispersion, ignition and jet fires, deflagrations, and detonations. In each Section, the BPG along with representative examples of applying them are presented. Some general guidelines for CFD simulations are given first.

¹ <http://support-cfd.eu> (accessed 16th June, 2017)

2.0 BEST PRACTICE GUIDELINES FOR HYDROGEN NUMERICAL SIMULATIONS

2.1 General BPG

Best Practice Guidelines relevant to all numerical simulations should be followed to ensure accuracy and credibility of CFD predictions. ERCOFTAC BPG [1] is a comprehensive document, which provides such guidelines for industrial simulations, many of which should be also applied in all FCH application simulations (dispersion, fire, detonation, etc.) and are summarized next.

Utilization of an adequately refined and high quality mesh is an important step in ensuring accuracy in numerical simulations. A number of parameters should be considered, such as resolution, expansion factor, cell aspect ratio and cell skewness. The choice of mesh resolution is to a large degree governed by the turbulence model employed in the simulation. Large Eddy Simulation (LES) require in general finer grids than Reynolds Averaged Navier-Stokes (RANS) type models.

The most appropriate grid density is estimated by a grid independency study. A grid independence study is very important because results with coarse grids can be misleading, as was demonstrated in [6]. For the grid independence study at least three different grid sizes should be tested. Ideally, each finer grid should have double the number of cells than the previous coarse one. In some cases this practice leads to prohibitively large mesh sizes, therefore is not always possible to follow. In these cases high refinement can be made only in regions of interest and in regions where high gradients are expected.

The size of the computational domain is another numerical parameter that should be carefully chosen. Domain boundaries should be located far enough from the areas of interest in order to minimize the impact of the boundary conditions on the results. For instance, in the case of hydrogen release in a vented room, the computational domain should be extended beyond the enclosure to avoid imposing boundary conditions at the opening. A domain size sensitivity study should be performed, in order to find the optimum extension.

A time step sensitivity study is also important. A constant time step can be used or Courant–Friedrichs–Lewy (CFL) number can be imposed to define the maximum time step. At least one simulation with a factor of two smaller time step/CFL number is recommended to ensure that the predictions remain the same. When LES is used, small time step sizes corresponding to CFL=1 are generally suggested.

Other parameters, such as the numerical scheme for discretization and turbulence models, are also critical. Laminar, RANS or LES models may be applied depending on the flow type in the region of interest. In general, high-order accuracy numerical schemes are recommended in order to decrease numerical diffusion, while in complex flows such as impinging jets and deflagrations they are considered as necessary. In LES, central differences schemes need to be used for the discretization of the convective term in the momentum equations because upwind-biased schemes suppress turbulence [7][8]. For the scalar conservation equation a Total Variation Diminishing (TVD) scheme should be used in order to ensure a bounded solution, i.e. mass fraction between 0 and 1. Finally, if the energy equation is solved, the same numerical scheme should be applied in both energy and mass fraction conservation equations, because they are strongly connected and convergence issues might arise.

2.2 BPG for release and dispersion simulations

Apart from the general Best Practice Guidelines, more specific guidelines should be followed in numerical simulations of hydrogen releases and dispersion. For grid generation, refinement should be imposed near the release point, where high concentration and velocity gradients are expected. The buoyant nature of hydrogen also requires fine grid resolution near the top boundary (ceiling) in case of indoor releases. For cryogenic hydrogen releases (e.g. liquid hydrogen) refinement on the ground is

important, as it is likely for the mixture to behave as a dense cloud near the spill point. In jet impingement simulations refinement should be imposed on the impact wall.

As far as the thermodynamic properties are concerned, the cubic Redlich-Kwong-Mathias-Copeman Equation of State (EoS) was suggested as the most appropriate for most applications connected with hydrogen and for the whole range of conditions (including saturated and supercritical) in [9]. The ideal gas approximation is accurate in ambient atmospheric conditions. Suitable correlations for saturation curves (required in two-phase simulations) as well as other specific physical properties (e.g. specific heats) can be found in [10] and [11]. The user should ensure that they have used the appropriate formula and constants which best fit within the temperature range of their problem.

For simulations of mixtures, the “ideal mixture” assumption can be made [3]. This requires the calculation of the mixture molecular viscosity if a solid phase is present in the mixture (e.g. when the humidity freezing is modelled in cryogenic releases). A solid phase has infinite viscosity, and therefore it should be treated carefully to prevent unphysically high values of mixture viscosity. One approach is to set the reciprocal of the mixture viscosity equal to the summation of the ratio of volume fraction to viscosity of each phase of each component [3]. In that approach infinite viscosity would result in zero contribution to mixture viscosity.

In modeling of hydrogen releases, a factor that greatly affects its dispersion is the hydrogen source boundary conditions. The source can be treated (depending on the software/code) in two basic ways: either as a volumetric source in one or more control volumes of the computational domain or as an area source located exactly at one of the faces of a given control volume. In the second approach the jet exit area (source area) could be either the full area of the face or a part of it, if the software/code allows part of the face to be “blocked” by defining the “face area porosity”. A source area approach is recommended for most cases because it is a more realistic implementation of the inlet boundary. However, in some cases, such as blowdown simulations [12], the volumetric source approach can be applied more easily.

In liquid hydrogen (LH₂) releases flashing occurs at the leak location, as the pressure drops from storage pressure to atmospheric resulting in two-phase mixtures. To estimate the flashed vapor fraction either isenthalpic or isentropic expansion can be assumed. Experience has shown that in case of low storage pressures (1-4 barg) the difference in the flashed vapor fraction between the two approaches is negligible, with the isentropic expansion predicting lower vapor fraction and consequently lower spill velocity.

One approach to model two phase flow is to assume that vapor and liquid phases are in thermodynamic and hydrodynamic equilibrium (i.e. share the same temperature, pressure and velocity), then solve the conservation equations for the mixture and a conservation equation for hydrogen (both vapour and liquid phase) and obtain the phase distribution using Raoult’s law. Another approach is to model the vaporization implicitly by solving an additional conservation equation for the vapor mass fraction [13]. Attention should be given to the coupling between phases (evaporation/condensation rates). An alternative approach is to separate the two-phase region from the vapour region [12]. Then a two-phase model (CFD or simpler model) could be applied within the two-phase region and a CFD model within the vapour region. The main difficulty in this approach is the separation of the two-phase and vapour regions and their interaction, while its advantage is that single phase (vapour) CFD simulations are faster compared to two-phase.

In cryogenic releases near ground (or water) the heat transfer from the ground (or water) is very important, see [14], [15], and should be considered. Solution of the temperature conservation (heat conduction) equation inside the ground to obtain the heat flux from the ground is required. Usually a transient one-dimensional equation with respect to depth inside the ground is solved. A grid independence study in the below-ground grid is recommended and fine grid resolution should be applied in the adjacent to the ground cells. Two types of boundary conditions can be used: (a) defined temperature and (b) heat balance at the interface. Experience has shown that during a liquefied release

on non pre-cooled ground, the temperature at the interface drops rapidly and thus it is reasonable to assume that the temperature at the interface is equal to the temperature of the adjacent dispersion cell and use the first type of boundary conditions. In cases with release above water, it is usually assumed that the water temperature remains constant and equal to its initial value. In this case film boiling is an important heat mechanism which must be accounted for.

In high-pressure jet releases, when the storage pressure is above 1.9 times the atmospheric pressure, the flow at the nozzle is choked. The pressure at the jet exit is above atmospheric (under-expanded jet) and expands to atmospheric at a short distance downstream through one or more expansion shocks. Several so called “notional nozzle” (or fictitious diameter) models were introduced to avoid detailed resolution of shock structures in highly compressible region close to the underexpanded jet nozzle and to lessen the computational effort. Performance of some notional nozzle approaches is compared in [16]. It was concluded that the Birch [17] and Schefer [18] approaches performed the best among the examined models. However, that study did not include notional nozzle models based on mass, momentum and energy conservation (such as [19], [20]) which are generally considered more accurate. For pressures above 10-20 MPa, notional nozzle approaches combined with ideal gas EoS are generally not recommended. Instead, approaches which use real gas EoS, such as the Schefer approach [18] that uses the Abel-Noble EoS, can be used. In [21] another notional nozzle theory is developed which combines Abel-Noble EoS with conservation of mass and energy. In cryogenic under-expanded jets approaches that assume temperatures in the notional nozzle equal to ambient temperature should be avoided.

In cryogenic hydrogen releases due to the low temperatures condensation and/or freezing of the ambient humidity and the nitrogen and oxygen component of air occurs resulting in two counteracting effects. The particles tend to decrease the buoyancy of the cloud, while the heat released during phase change tends to increase the buoyancy of the cloud. If the generated particles become large enough they might start falling to the ground, violating of the hydrodynamic equilibrium approach. In this case one could use slip (or drift) CFD models, [22].

For the evaluation of dispersion models, use of statistical performance measures (SPMs) is recommended. Narrower acceptable ranges for the SPMs in indoor release are also suggested compared to outdoor releases [5]. SPMs may also be used to evaluate the performance of models in other areas, (e.g. deflagration modelling) but there is less experience of their use in these areas.

2.2.1 Example case: cryogenic sonic jet simulation

A cryogenic sonic jet simulation [23] is presented here as an example following the recommended BPG, while a more detailed example with subsonic hydrogen jet can be found in [5]. The simulations were performed by NCSRD based on the KIT-2011 experiments [24], which involve horizontal hydrogen jet releases in closed facility. The storage conditions varied in the tests; however, all of them corresponded to either vapor or supercritical state.

For the simulations the recommended BPG were followed: the computational domain was extended far enough from the release point and three different grid sizes were examined to assess the effect of grid size. Two different CFL numbers were applied to restrict the maximum time step having no impact on the results. A 3rd order numerical scheme (QUICK) was used for the convective terms. To model the under-expanded jet a notional nozzle approach was employed, which performs mass and momentum balance between the actual and the notional nozzle similar to the approach of Birch [17], but assumes that the temperature at notional nozzle is equal to the nozzle temperature. An isentropic energy balance between the nozzle and a notional nozzle as used in [19] and [20] would produce a temperature at the notional nozzle lower than at the actual nozzle and possibly in the two-phase region resulting in a more complex simulation. Therefore, such an approach was avoided, in order to reduce the computational cost. Finally, for the turbulence modeling the k- ϵ model was employed. The comparison with the experiment is presented in Figure 1 and shows that good agreement is achieved with the predictions tending to slightly overestimate the concentrations.

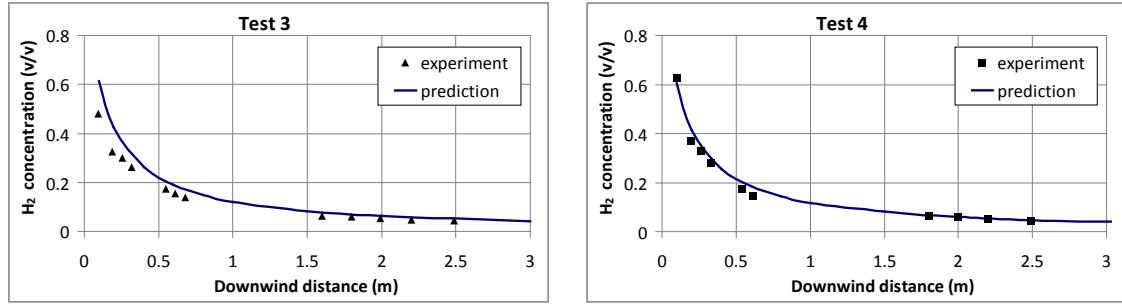


Figure 1. Comparison of the simulation results with the experimental results in cryo-compressed hydrogen jet.

2.3 BPG for Ignition and Jet fire simulations

A sudden release of hydrogen gas from a high pressure reservoir often leads to the so - called spontaneous diffusion ignition phenomenon. Numerical modelling of hydrogen autoignition presents significant computational challenges. The consensus among researchers is presently turning toward shock heating as the primary cause of hydrogen spontaneous ignition. This means that numerical methods seeking to model autoignition have to be able to simulate shocks, small scale turbulent mixing and shock wave/vortex interactions. In practical terms, it means that the ignition model would require a combination of highly resolved mesh with highly accurate numerical method. Many researchers sought to avoid prohibitively high computational resource requirements by reducing the problem to two or even one dimension. 2-D models provide an opportunity to perform simulations of more realistic release scenarios, which can be directly compared with experimental data. The importance of shock wave interaction and small scale turbulent mixture processes encouraged many researchers to choose a Direct Numerical Simulation (DNS) approach. Despite the 2-D approximation, a large number of control volumes are required. Most DNS simulations of hydrogen autoignition utilize meshes with resolution on order of 15-20 μm with overall number of control volumes in millions or tens of millions and relatively small computational domains. DNS simulations usually use highly detailed chemical kinetics for modelling of combustion processes. An alternative approach is to utilize LES, which allows modelling of significantly larger and more complex geometries and reduces the necessary computational resources. A shortcoming of all 2-D models, in addition to being limited to simplified axi-symmetrical geometry, is compromised simulation of turbulence, which is an inherently 3-D phenomenon. Fully 3-D approaches allow researchers to both capture the appropriate physics of turbulent mixing and to investigate more realistic geometries such as Pressure Relief Devices (PRDs) [25]. Since performing 3-D DNS would be prohibitively expensive, 3-D LES with accurate combustion models is preferred, such as Eddy Dissipation Concept (EDC) plus detailed chemistry, compensating for the inevitably more coarse mesh.

Jet fire modelling presents a different set of challenges compared to ignition modelling. While typically presenting less stringent requirements for mesh resolution and accurate handling of strong shocks, jet fires, particularly originating from under-expanded jets, often present a problem with a very wide range of scales. Indeed, on one hand the release origin is typically measured in millimeters, and in case of under-expanded supersonic release may require large number of CV across the nozzle to properly capture flow dynamics and shock structure. On the other hand, jet fires often extend for many meters, requiring employment of a very large domain. As a result the notional nozzle approach (which is used in dispersion simulations) may also be applied here. Regarding turbulence, jet fires are usually modelled using LES or RANS approaches. It should be noted that virtually all combustion occurs at subgrid scales, since there are practically no resolved combustion reactions. A wide range of combustion models can be used, from simplified Eddy Break-Up (EBU) / Eddy Dissipation Model (EDM) to flamelet and EDC with detailed chemistry, depending on the problem conditions and requirements. More precise models such as EDC can provide more accurate modelling of physical phenomena at the expense of significantly larger computational requirements. The choice of the combustion model should also be determined by specific phenomena to be simulated. EBU is

primarily limited to modelling of well-ventilated fires. It is not suitable for simulation of phenomena such as flame lift-off fires due to its underlying assumption of chemical rates being much faster than the mixing/flow rates. The flamelet approach provides slightly better treatment of chemistry. Accurate modelling of under-ventilated fires requires consideration of chemical kinetics [26].

2.3.1 Example case: spontaneous ignition in PRD

Simulation of a spontaneous ignition in a pressure relief device [25] will be described briefly here, while three representative jet fire simulations are demonstrated in [26],[27],[28]. The hydrogen was released from a high pressure system into a channel ending in a T-shaped nozzle mimicking a PRD (Figure 2). The high-pressure system consisted of a 210 mm long tube with 16 mm internal diameter followed by a 280 mm long tube with 10 mm diameter at the end of which was a flat burst disk, made from a soft metal with cuts to facilitate failure. On the other side of the burst disk was a simulated PRD open to atmosphere. Spontaneous ignition was observed during the experiment at a pressure of 2.43 MPa.

The computational domain and mesh are illustrated in Figure 2. A hybrid mesh (tetrahedral and hexahedral cells) consisting of 417,685 cells was used. The cells have a size of 400 μm at the PRD's axial channel and cross-sections, and 200 μm at the intersection area. The non-instantaneous burst disk opening plays an important role in the process of ignition due to effect on mixing between hydrogen and air. The opening of a membrane was therefore approximated in simulations by a step-like process of consecutive opening of 10 concentric sections (Figure 2). For the discretization of the convective terms a second order upwind Advection Upstream Splitting Method (AUSM) method was used. For the temporal discretization explicit scheme was chosen with CFL number equal to 0.2.

The simulation employed LES with a set of filtered 3-D compressible equations for conservation of mass, momentum, energy and species. The renormalization group (RNG) theory was used as a sub-grid-scale model to calculate the effective viscosity. For the combustion, the EDC model was used with updates incorporating detailed Arrhenius chemical kinetics in turbulent flames as the combustion sub-model. The EDC model expression for a combustion rate was based on an assumption that chemical reactions occur in the small scale structures on the Kolmogorov's scale where the dissipation of turbulence energy takes place. A detailed 21-step chemical reaction mechanism of hydrogen combustion in air employing 37 elementary reactions was used.

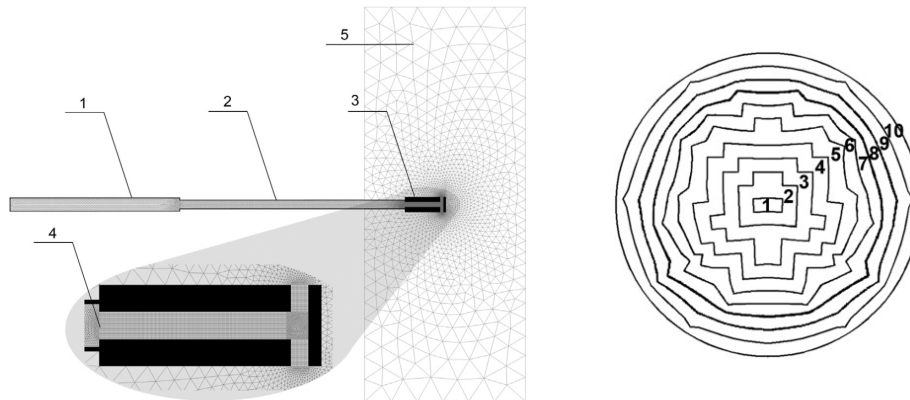


Figure 2. Left: View of the computational domain (1,2: high pressure tubes, 3: PRD, 4: burst disk, 5: external domain). Right: Step-like approximation of a burst disk rupture process.

Numerical simulations were performed for various initial hydrogen pressures. For the cases with 1.35 and 1.5 MPa initial pressure no auto-ignition was detected whereas at storage pressures 1.65 and 2.43 MPa an ignition followed by a self-extinction of reaction was observed. For the case with initial pressure 2.9 MPa, the ignition was observed at approximately 62 μs at the location of the leading shock wave secondary reflection. The fact of ignition and its location can be confirmed by sudden appearance of large quantities of hydroxyl OH and temperature (Figure 3).

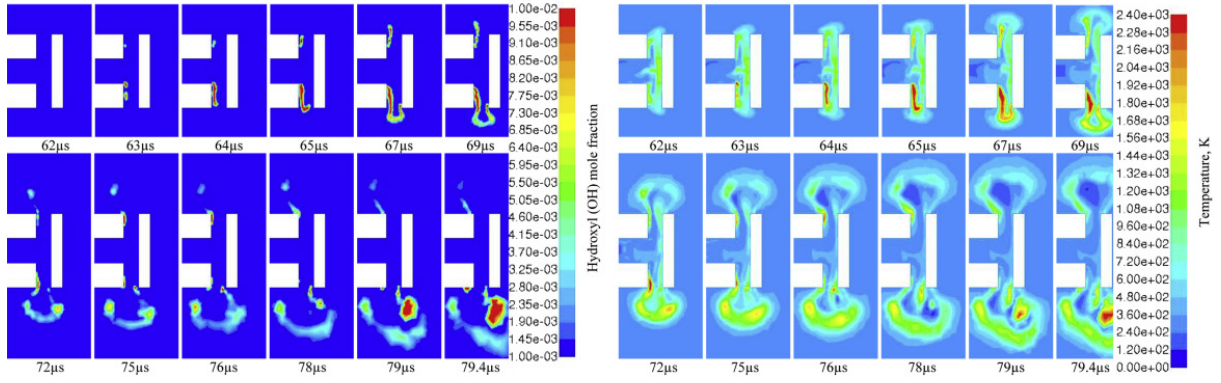


Figure 3. OH concentration (left) and temperature (right) contours at the axis of the PRD for the case with 2.9 MPa initial pressure.

2.4 BPG for Deflagration simulations

The modelling of deflagrations remains a challenge. The reasons are rooted in the complex interactions between the turbulent flow field and combustion chemistry, together with the very wide-range of applications for which models are required. In the open atmosphere, combustion of an initially quiescent mixture of hydrogen and air begins as a laminar flame. A cellular flame structure soon develops. However, this cellular structure rapidly breaks down into a self-similar regime of turbulent flame propagation when the flame front reaches a radius of about 1 m. Initial turbulence and wind can also affect flame propagation. In confined but vented deflagrations, the physics tend to be more complex - largely due to a number of flow-combustion instabilities. Of particular relevance are the Rayleigh-Taylor instability at the vent exit and, potentially, flame-acoustic interactions. If the flame encounters obstacles its rate of propagation can be greatly increased; due to the acceleration of the flow between and around obstacles - with a consequent increase in turbulence and thus flame surface area. This results in a positive feedback between the rate of combustion and flow turbulence, leading to ever greater rates of flame propagation and eventually the possibility of transition from deflagration to detonation. More details on the physics of hydrogen deflagrations, and the difficulties which these physics pose for CFD models, are given in [12].

The choice of combustion model for the estimation of the mean reaction rate is important. The reaction rate has strong effect on the deflagration process development and as a result it needs to be predicted with accuracy. Various combustion models have been used in the literature. Guidance provided by code vendors and developers must be followed. Comparison of many of these models have been made against hydrogen deflagration, e.g. in [29], [30]. The overall conclusion from these comparisons is that, unfortunately, there is no one modelling approach which is clearly superior to all others and applicable to all circumstances. A significant drawback of many of the models is the uncertainty of constants' values. The values of model constants recommended by code developers should be used, unless otherwise indicated by research which is directly relevant to the FCH application being modelled.

Necessary key-characteristics of combustion models can be defined according to the physical characteristics of each case. In large scale deflagrations, the model should be capable of addressing the self-similar flame acceleration which is experimentally observed. In vented deflagration the model should be capable of reproducing the violence of the external explosion, for example by incorporating a sub-model for the Rayleigh-Taylor instability [31]. In the case of high congestion, the effects of the obstacles should be account for. This is a considerable challenge, as they can be too numerous and/or too small to be able to be resolved directly with the mesh. The approach which is usually taken is to include sub-models to account for their influence, often referred to as PDR – Porosity Distributed Resistance. The PDR approach has been most commonly-used within the context of RANS modelling of deflagrations [32]. However, PDR approaches can rely heavily on calibration against test data, so

there is uncertainty when they are applied outside the range of known validation cases. Therefore the code-vendor guidelines should be applied in that case.

There appears to be a large difference in complexity between experiments used to validate and guide the development of hydrogen deflagration models, and FCH applications. For instance, the former are usually undertaken with homogenous hydrogen-air mixtures, often at stoichiometric conditions and often with quiescent initial conditions. However, in FCH applications, releases of hydrogen are often from high pressure sources, leading to high initial turbulence and a markedly non-uniform distribution of hydrogen – in which concentrations can range from 100% to 0%. In other circumstances, stratified flows and layering can occur. Therefore, in practice, releases of hydrogen often do not result in fully pre-mixed conditions. It should not be assumed that models which have been demonstrated to be valid for uniform and/or stoichiometric conditions are also valid in general for non-uniform/lean mixtures.

However, if models are to be used in risk assessments, rather than just compared against validation cases, account will regularly need to be taken of highly non-uniform initial conditions. The highly non-uniform concentration field resulting from a realistic release of hydrogen should be post-processed to an equivalent uniform stoichiometric volume before deflagration modelling is undertaken - unless the deflagration model has been specifically validated for such non-uniform conditions. Examples of this approach are the works of Hansen et al. (2013) [33] and Middha & Hansen (2009) [34]. There are a number of means by which this conversion can be undertaken [33], leading to greater or lesser conservatism in the size of the equivalent stoichiometric cloud. The method used to undertake this conversion to an equivalent uniform stoichiometric volume should be conservative, i.e. err on the side of caution.

2.4.1 Example case: vented deflagration

Two representative examples of deflagration simulations conducted based on BPG are presented in [30] and [35]. Here, the vented deflagration simulation conducted by HSE of the FM-Global experiment is presented. The experimental facility consisted of a square-floored enclosure of 4.6×4.6×3.0 m with a 5.4 m² square vent located in the center of one of the walls. Homogeneous 18% v/v hydrogen-air mixture filled the room and was ignited at its center. Two CFD codes were used, ANSYS CFX and GexCon FLACS. The CFX simulations were carried out using tetrahedral meshes whereas a Cartesian mesh was used in FLACS. Turbulence was modelled using the k-ε turbulence model. In CFX combustion was modelled using the Zimont turbulent flame speed correlation. Sensitivity studies were conducted as was suggested in the BPG to test the effect of the computational domain size, the mesh resolution and the initial turbulence conditions.

FLACS predictions were seen to be sensitive to the choice of domain size while both the FLACS and CFX predictions were sensitive to the mesh resolution and initial turbulence conditions. The fact that these sensitivities exist highlights the value in following BPGs and carrying out sensitivity analyses. By carrying out sensitivity analyses it is possible to build confidence and trust in CFD predictions. For both FLACS and CFX, it was possible to use a sufficiently large computational domain to obtain computational domain size independent results. Similarly, it was possible to use a sufficiently high mesh resolution to obtain reasonably mesh independent results. Although full mesh independence was not achieved for both the over-pressure and the flame speed predictions, the level of mesh sensitivity at the higher resolution meshes was relatively small. While it was possible to achieve computational domain size independent results and a reasonable level of mesh independence, it was not possible to obtain results that were independent of the initial turbulence conditions. The initial turbulence conditions were seen to have a significant effect on both the FLACS and CFX predictions.

HSE's final set of simulations were carried out with initial turbulence conditions specified according to advice from the code vendors. Both the FLACS and CFX final simulations gave predictions that were in reasonable or good agreement with the FM Global measurements, as is shown in Figure 4. However, more work is required to confirm the wider applicability of these modelling approaches.

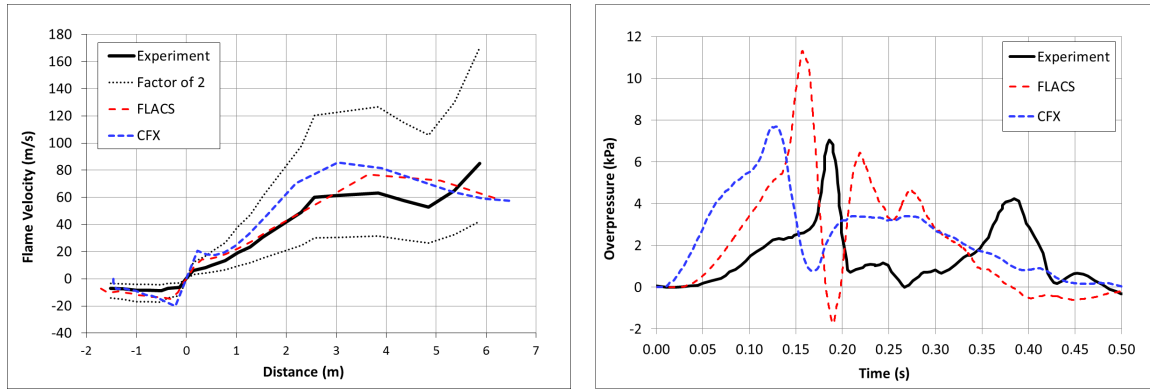


Figure 4. Flame speed (left) and over-pressure (right) predictions from the CFD simulations.

2.5 BPG for Detonation simulations

Among different accident scenarios detonation is often considered as the ‘worst case’ scenario, and therefore, in safety analysis detonation modelling should be considered. For steady state detonation a set of conservation equations in Euler formulation and a model of chemical interaction are necessary and sufficient in most cases. Often the selection of the chemical interaction model plays a key role in the successful implementation and utilization of the detonation model. In more complex cases such as, e.g., transient regimes of detonation, deflagration-to-detonation transition, interaction with obstacles, shock reflections, flames, etc. utilization of the Navier-Stokes equations, as well as modelling of turbulence, could be required for adequate reproduction of the relative phenomena.

Models which rely on resolving the flame front have prohibitively high computational cost for use on practical applications because a large number of cells must be placed in the reaction zone. Moreover, detailed chemistry modelling may also be required. Two models which have been applied successfully in large scale detonation simulations are the Heaviside detonation model developed by Karlsruhe Institute of Technology [36] and the LES detonation model developed by Ulster University [37]. In both models the reaction zone length is artificially increased in order to be resolved by several computational cells. In the first model an Arrhenius-like chemical reaction rate is used which provides the necessary species consumption rate in a fully developed steady-state detonation. In the second model the progress variable equation is used for modelling the reaction front propagation. The source term is modelled with the gradient method, based on a product of pre-shock mixture density and the detonation velocity. Chemical kinetics enter the combustion model only through their influence on the detonation velocity and modelling of detailed chemistry is omitted.

More specific BPG depend on the particular application. Simulation of detonation in a real scale geometry is presented in [36]. Two other example cases are presented next in summary.

2.5.1 Example case: detonation cells

One of the most important characteristics of detonation is its cellular structures. The cell width of the detonation front in 30% v/v hydrogen-air mixture is around 12 mm. To reduce computational efforts, the detonation cellular structure reproduced in 2-D. A simple rectangular region was filled with a hydrogen-air mixture of 30% v/v. In order to initiate the detonation a high pressure (100 bar) and temperature (3000 K) region was defined. To reproduce the detonation cellular structures, 40 to 50 control volumes are usually necessary to discretize one detonation cell. As a result a resolution of 0.3 mm was used. To reduce the computational effort the technique of adaptive local mesh refinement was used. A view of the grid at the area of the flame front is shown in Figure 5. Two levels of grid refinement were used, the first level of 1 mm resolution and the finer level of 0.25 mm. The first level covers the region of length equal to approximately two and half detonation cell behind the shock front and the second region covers the region of length equal to half detonation cell in front of the shock front. In grid regeneration the balance of computational cost and grid regeneration is important. Finer

regions should not be too small otherwise the frequent grid regeneration and data redistribution could reduce the code efficiency.

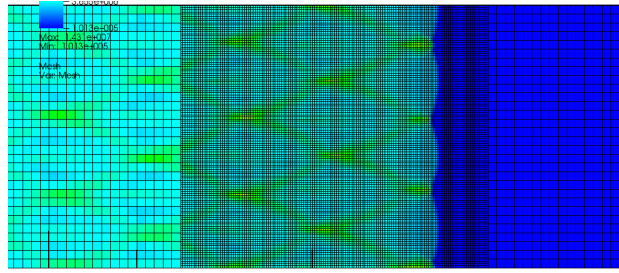


Figure 5. Local mesh refinement in the simulation of detonation's cellular structures.

The simplified Euler equations were solved and the one step Arrhenius method was used for combustion. Figure 6 shows the numerically emulated smoked-foil records (maximum pressure records at each cell in the simulation process) at different times. At approximately half the length of the domain (0.5 m) the cellular structures are generated. Cellular structures grow as the detonation wave propagates, starting from 7 mm width and reaching the experimental width of 12 mm at the final stage. The reason for not capturing the correct cell size at the initial stage is that a self-sustained stable detonation wave has not been reached due to the numerical details of the detonation wave initialization. A grid independence study was conducted and showed that the 0.25mm resolution is enough for the simulation of hydrogen-air detonation cells. A grid of 0.5 mm base level resolution and 0.0312 mm fine level were also tested. The only difference in this simulation was that the smoked-foil structure appeared earlier. The reason for this is that in high resolution the perturbations which are responsible for this structure can amplify more quickly.

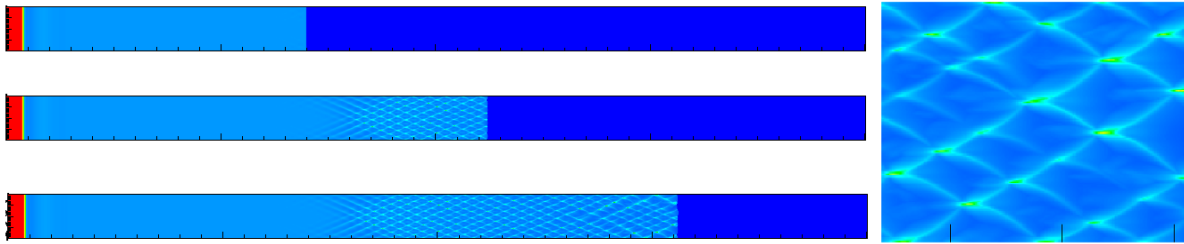


Figure 6. Smoked-foil records at different times (left) and cellular structures (right).

2.5.2 Example case: DDT

Deflagration to Detonation Transition (DDT) is a phenomenon in combustion, which is very important to hydrogen safety analysis. The simulated experiment was the MINI RUT with the experimental ID mr046 from [38]. The experiment involved stoichiometric hydrogen-air mixture in an obstructed channel (cross section 45×50 mm) followed by a chamber. The ignition point was located at the beginning of the channel. The geometry of MINI RUT is quite complicated. However, the numerical reproduction of DDT phenomena does not require reconstructing the whole facility. In the experiment, deflagration transitioned to detonation at the end of the obstructed channel. Therefore, only the obstructed channel was simulated, as shown in Figure 7. As a result, much higher resolution can be used in the computational domain. A uniform structured Cartesian grid was used consisting of 18 million cells. For the spacial and time discretization a 2nd order explicit Total Variation Diminishing (TVD) scheme [39] and the 2nd order Runge-Kutta method was used. A CFL restriction of 0.9 was imposed. For DDT simulation, the chemical model plays an important role so in the numerical reproduction of the experiment, the hybrid DDT chemical reaction model was used. This model utilizes two combustion rates, a combustion rate due to deflagration process and a combustion rate due to detonation [5]. For turbulence the LES methodology was used along with the Smagorinsky-Lilly sub-grid model.

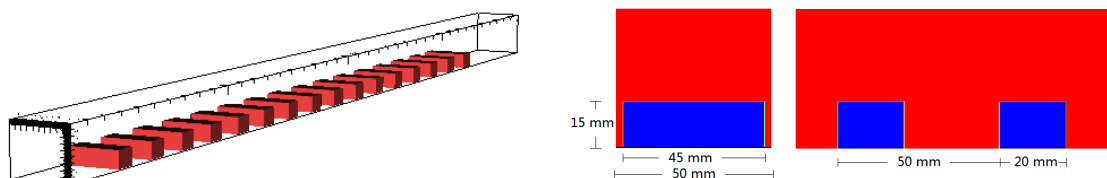


Figure 7. View of the computational domain (left) and YZ, XY near-views of the obstacles (right).

In the numerical simulation, the deflagration transitions to detonation around the last obstacle of the channel which is in good agreement with the experiment. Figure 8 presents the predicted and the experimental overpressure time series at two sensors. The simulation over-estimates the experiment, however, the pressure curve has the same trend as in the experiment. Moreover, the propagation speed of the pressure wave in numerical simulation was almost the same as in the experiment. Consequently, the simulation was regarded as a successful reproduction of the experiment.

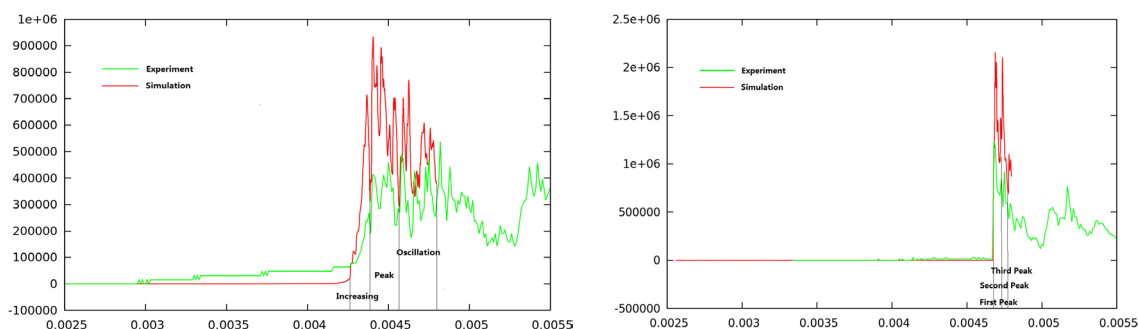


Figure 8. Comparison of pressure records at 0.47 and 0.79 m from the ignition point.

3.0 CONCLUSIONS

In this paper, the BPG in numerical simulations for Fuel Cells and Hydrogen applications were briefly presented. The BPG were developed within the SUSANA project and are one of the main outputs of the project. These BPG focus on the practical needs of engineers in consultancies and industry undertaking CFD simulations in support of hazard/risk assessments of hydrogen facilities, and the needs of regulatory authorities. BPG application through a series of CFD example cases were also presented for each phenomenon (dispersion, combustion and detonation), in order to provide a demonstration of their application.

ACKNOWLEDGEMENTS

The authors would like to thank the Fuel Cell and Hydrogen Joint Undertaking for the co-funding of the project SUSANA (Grant agreement FCH-JU-325386). The Health and Safety Executive (HSE) co-funded the contribution by its researchers. Its contents, including any opinions and/or conclusions expressed, are those of the authors alone and do not necessarily reflect HSE policy.

REFERENCES

1. Casey, M. and Wintergate, T., Special interest group on quality and trust in industrial CFD – Best Practice Guidelines, *ERCOTAC*, 2000.
2. Franke, B., Hellsten, J., Schlünzen, A. and Carissimo, H., COST Best practice guidelines for the CFD simulation of flows in the urban environment, 2007.
3. SUSANA D3.2, Deliverable 3.2, Guide to best practices in numerical simulations (Report of the SUSANA project, funded by Fuel Cells and Hydrogen Joint Undertaking (FCH JU). Grant agreement No. 325386), 2016.
4. SUSANA D5.2, Deliverable 5.2, Report on model benchmarking exercise 1, 2016.
5. SUSANA D5.3, Deliverable 5.3, Report on model benchmarking exercise 2, 2016, pp. 1–101.

6. Koutsourakis, N., Tolias, I.C., Venetsanos, A.G. and Bartzis, J.G., Evaluation of an LES code Against a Hydrogen Dispersion Experiment, *CFD Letters*, **4**, No. 4, 2012, pp. 225–236.
7. Mittal, R., and Moin, P., Suitability of Upwind-Biased Finite Difference Schemes for Large-Eddy Simulation of Turbulent Flows, *AIAA J.*, **35**, No. 8, 1997, pp. 1415–1417.
8. Breuer, M., Large eddy simulation of the subcritical flow past a circular cylinder: numerical and modeling aspects, *Int. J. Numer. Methods Fluids*, **28**, No. 9, 1998, pp. 1281–1302.
9. Nasrifar, K., Comparative study of eleven equations of state in predicting the thermodynamic properties of hydrogen, *Int. J. Hydrogen Energy*, **35**, No. 8, 2010, pp. 3802–3811.
10. NIST, <http://webbook.nist.gov/>.
11. Poling, B.E. and Prausnitz, M., *The Properties of Gases and Liquids*, 5th edition, 2004.
12. SUSANA D2.1, Deliverable D2.1, Review: State-of-the-art in physical and mathematical modelling of safety phenomena relevant to FCH technologies, 2016.
13. Jin, T., Wu, M., Liu, Y., Lei, G., Chen, H. and Lan, Y., CFD modeling and analysis of the influence factors of liquid hydrogen spills in open environment, *Int. J. Hydrogen Energy*, **42**, No. 1, 2017, pp. 732–739.
14. Verfondern, K., Safety Considerations on Liquid Hydrogen, Report, Jülich Forschungszentrum, 2008.
15. Statharas, J.C., Venetsanos, A.G., Bartzis, J.G., Würtz, J. and Schmidtchen, U., Analysis of data from spilling experiments performed with liquid hydrogen, *J. Hazard. Mater.*, **77**, No. 1–3, 2000, pp. 57–75.
16. Papanikolaou, E. and Baraldi, D., Evaluation of notional nozzle approaches for CFD simulations of free-shear under-expanded hydrogen jets, *Int. J. Hydrogen Energy*, **37**, No. 23, 2012, pp. 18563–18574.
17. Birch, A.D., Hughes, D.J. and Swaffield, F., Velocity decay of high pressure jets, *Combust. Sci. Technol.*, **45**, 1987, pp. 161–171.
18. Schefer, R.W., Houf, W.G., Williams, T.C., Bourne, B. and Colton, J., Characterization of high-pressure, underexpanded hydrogen-jet flames, *Int. J. Hydrogen Energy*, **32**, No. 12, 2007, pp. 2081–2093.
19. Xiao, J., Travis, J.R. and Breitung, W., Hydrogen release from a high pressure gaseous hydrogen reservoir in case of a small leak, *Int. J. Hydrogen Energy*, **36**, No. 3, 2011, pp. 2545–2554.
20. Yüceil, K. and Öttügen, M., Scaling parameters for underexpanded supersonic jets, *Phys. Fluids*, **14**, No. 12, 2002, p.p. 4206.
21. Molkov, V.V., Fundamentals of hydrogen safety engineering, Vol.1, Bookboon, ISBN 978-87-403-0226-4, 2012, pp.216.
22. Giannissi, S.G., Venetsanos, A.G., Markatos, N. and Bartzis, J.G., CFD modeling of hydrogen dispersion under cryogenic release conditions, *Int. J. Hydrogen Energy*, **39**, No. 28, 2014, pp. 15851–15863.
23. Venetsanos, A.G., Giannissi, S.G., Release and dispersion modeling of cryogenic under-expanded hydrogen jets, *Int. J. Hydrogen Energy*, 2016, in press.
24. Vesper, A., Kuznetsov, M., Fast, G., Friedrich, A., Kotchourko, N., Stern, G., Schwall, M. and Breitung, W., The structure and flame propagation regimes in turbulent hydrogen jets, *Int. J. Hydrogen Energy*, **36**, No. 3, 2011, pp. 2351–2359.
25. Bragin, M.V., Makarov, D.V. and Molkov, V.V., Pressure limit of hydrogen spontaneous ignition in a T-shaped channel, *Int. J. Hydrogen Energy*, **38**, No. 19, 2013, pp. 8039–8052.
26. Molkov, V., Shentsov, V., Brennan, S. and Makarov, D., Hydrogen non-premixed combustion in enclosure with one vent and sustained release: Numerical experiments, *Int. J. Hydrogen Energy*, **39**, No. 20, 2014, pp. 10788–10801.
27. Brennan, S.L., Makarov, D.V. and Molkov, V., LES of high pressure hydrogen jet fire, *J. Loss Prev. Process Ind.*, **22**, No. 3, 2009, pp. 353–359.
28. Makarov, D. and Molkov, V., Plane hydrogen jets, *Int. J. Hydrogen Energy*, **38**, No. 19, 2013, pp.

8068–8083.

29. Makarov, D., Verbecke, F. and Molkov, V., An inter-comparison exercise on CFD model capabilities to predict a hydrogen explosion in a simulated vehicle refuelling environment, *Int. J. Hydrogen Energy*, **34**, No. 6, 2009, pp. 2800–2814.
30. Tolias, I.C., Stewart, J.R., Newton, A., Keenan, J., Makarov, D., Hoyes, J.R., Molkov, V. and Venetsanos, A.G., Numerical simulations of vented hydrogen deflagrations in a medium-scale enclosure, *Journal of Loss Prevention in the Process Industries*, 2017, under review.
31. Keenan, J.J., Makarov, D.V. and Molkov, V.V., Rayleigh–Taylor instability: Modelling and effect on coherent deflagrations, *Int. J. Hydrogen Energy*, **39**, No. 35, 2014, pp. 20467–20473.
32. Hansen, O.R., Renoult, J., Sherman, M.P. and Tieszen, S.R., Validation of FLACS-Hydrogen CFD consequence prediction model against large scale H₂ explosion experiments in the FLAME facility, in *Int. Conf. on Hydrogen Safety*, 2005.
33. Hansen, O.R., Gavelli, F., Davis, S.G. and Middha, P., Equivalent cloud methods used for explosion risk and consequence studies, *J. Loss Prev. Process Ind.*, **26**, No. 3, 2013, pp. 511–527.
34. Middha, P. and Hansen, O.R., CFD simulation study to investigate the risk from hydrogen vehicles in tunnels, *Int. J. Hydrogen Energy*, **34**, No. 14, 2009, pp. 5875–5886.
35. Tolias, I.C., Venetsanos, A.G., Markatos, N. and Kiranoudis, C.T., CFD evaluation against a large scale unconfined hydrogen deflagration, *Int. J. Hydrogen Energy*, 2016, in press.
36. Yáñez, J., Kotchourko, A., Lelyakin, A., Gavrikov, A., Efimenko, A., Zbikowski, M., Makarov, D. and Molkov, V., A comparison exercise on the CFD detonation simulation in large-scale confined volumes, *Int. J. Hydrogen Energy*, **36**, No. 3, 2011, pp. 2613–2619.
37. Zbikowski, M., Makarov, D. and Molkov, V., LES model of large scale hydrogen–air planar detonations: Verification by the ZND theory, *Int. J. Hydrogen Energy*, **33**, No. 18, 2008, pp. 4884–4892.
38. Matsukov, D., Kuznetsov, M., Alekseev, V. and Dorofeev, S.B., Photographic study of transition from fast deflagrations to detonations, in *22nd International Symposium on Shock Waves*, 1999, pp. 195–200.
39. Harten, A., High resolution schemes for hyperbolic conservation laws, *J. Comput. Phys.*, **49**, No. 3, 1983, pp. 357–393.